# Phonon-induced exciton spin relaxation in semimagnetic quantum wells

E. Tsitsishvili* and R. v. Baltz
*Institut für Theorie der Kondensierten Materie, Universität Karlsruhe, D-76128 Karlsruhe, Germany*

H. Kalt
*Institut für Angewandte Physik, Universität Karlsruhe, D-76128 Karlsruhe, Germany*
(Received 20 October 2004; revised manuscript received 22 December 2004; published 26 April 2005)

Theoretical results are given for spin relaxation in semimagnetic semiconductor quantum wells due to longitudinal optical (LO) phonon-induced flips of exciton spins at zero temperature and modest magnetic fields. Relaxation in this scenario is due to spin-flip transitions within the heavy-hole exciton subbands which are mediated by the coupling of excitonic spin states via the electron-hole exchange interaction. Relaxation rates are found to depend strongly on a magnetic field, exciton momentum, and size of the quantum well. Results are illustrated by evaluations for the ZnSe-based semimagnetic quantum wells. In longitudinal magnetic fields (Faraday geometry) a maximum in the relaxation rate is found for zero-momentum excitons at a Zeeman splitting of $\sim$60 meV. In transverse magnetic fields (Voigt geometry) the LO-induced spin relaxation is strongly suppressed.

DOI: 10.1103/PhysRevB.71.155320 PACS number(s): 72.25.Rb, 63.20.Ls, 75.50.Pp, 78.67.De

## I. INTRODUCTION

The achievements in spin injection technology with the possibility of successful spin functionality for diluted magnetic semiconductors (DMS's) (see Refs. 1–3 and references therein), have renewed interest in the study of the spin relaxation of electrons and holes. The required techniques for such investigations are given by methods of ultrafast spectroscopy which allow to observe the electron and hole spin kinetics in semiconductor quantum structures over a wide range of temperatures and magnetic fields.[4–11] Also the theory of the electron (hole) spin relaxation is well established in terms of the (*sp-d*) exchange scattering by magnetic ions.[12–15]

Since some prominent proposals[16] for the achievement of spin-based information processing are based on optical generation, detection or control of spin states, one needs to consider the dynamics of *excitonic* spins in particular also in DMS structures. Experimental measurements of the exciton spin relaxation times are performed by various groups in different DMS systems. Exciton-spin relaxation times of order tens of picoseconds, for example, were observed for the CdTe- and ZnSe-based quantum wells (QW's).[17,18] A strong increase in the spin lifetime, however, was found in the ZnSe-based strained epilayers and quantum wells.[19–21] Recent experimental findings in Refs. 22 and 23 indicate a direct involvement of longitudinal optical (LO) phonons in the exciton spin-relaxation in CdSe/ZnMnSe superlattices and ZnMnSe DMS layers. In spite of intensive work, the exciton spin-relaxation processes are still not fully understood. One of the reasons is a deficiency in the present theory. The exception is the exchange-induced precession mechanism leading to exciton spin-relaxation in quantum wells (QWs).[24] But this mechanism cannot be directly applied to the case of semimagnetic QWs with a giant spin splitting.[22]

For excitons there are two channels to change its spin. The first one is due to an independent change in the electron and hole spin—a two-step relaxation process. The second one is a result of simultaneous flips of electron and hole spins—the direct exciton spin-flip process. For the former case, the magnetic exchange mechanism can still be efficient and the exciton spin-relaxation rate is controlled by the slowest step. For example, a short electron spin lifetime of $\tau_e \sim 4$ ps was estimated theoretically in Ref. 22 for a 10 nm (strained) ZnMnSe QW, and a few times longer spin lifetime is obtained in this case for holes.[10,25] For the latter case, the exciton spin and energy change simultaneously and therefore a direct exciton spin-flip process occurs by the phonon participation. Actually, this relaxation channel was discussed as a possible process for observed spin relaxation in Ref. 22. But, such a process was viewed as a high order process requiring some magnetic mediator between the LO phonons and the carrier spins.[22]

Our aim is to give a microscopic model calculation for direct spin-flip transitions within exciton subbands including the dependence on an external magnetic field. The basic mechanism is the Maialle-Andrada-Sham (MAS)[24] mechanism of the electron-hole exchange interaction in QWs. This interaction is responsible for the coupling between the heavy-hole (*hh*) exciton spin states with a finite center-of-mass momentum and allows direct transitions between the spin-split excitonic branches by a spin-independent perturbation. We shall limit our consideration to the exciton interaction with LO phonons. We will show that the proposed mechanism is able to explain qualitatively experimental findings in Refs. 22 and 23. This spin relaxation is actually rather efficient and is thus able to compete with the above mentioned mechanism related to the magnetic exchange. We also discuss some possibilities to verify experimentally both the magnetic exchange and the exciton exchange spin-relaxation models.

## II. RELAXATION RATE

We consider semimagnetic semiconductor quantum well (QW) structures where we first assume that the *sp-d* ex-

 

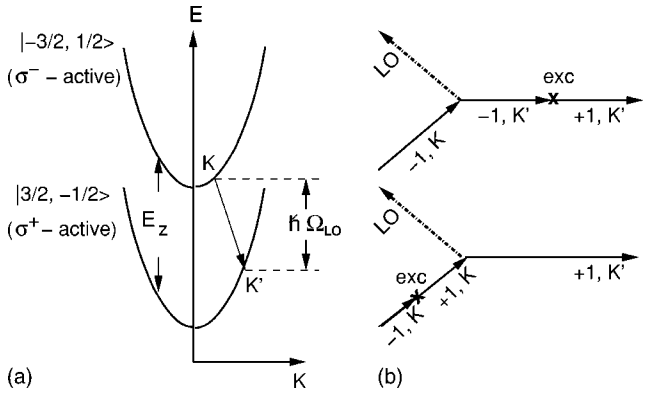


FIG. 1. Schematic diagram showing (a) the LO phonon-induced transition within the spin-split bands of the *hh* exciton and (b) the second-order processes involved Eq. (2).

change interaction results in large $g$ factors for the electron and hole spins. For moderate magnetic fields, it becomes possible to observe the Zeeman splitting, whereas the field-induced changes of the subband wave functions and energies can still be neglected. We calculate the relaxation rate for the (direct) spin-flip transitions within the *hh* exciton subbands which are split by an external magnetic field. These transitions are accompanied by the energy relaxation to the phonon bath, whereas the coupling of exciton spin states by the MAS interaction is viewed as a perturbation.

For zinc-blend semiconductor QWs, the structure of excitons is well known.[26] The single-particle basis from which the *hh* exciton is constructed consists of a heavy hole with spin $J_h=3/2$, $J_{h,z}=\pm 3/2$, and an electron with spin $s=1/2$, $s_z=\pm 1/2$ (the $z$ direction is chosen to point along the quantum well growth direction). From these states four exciton states are formed which are characterized by their angular momentum projections $S_z=s_z+J_{h,z}$. States with $|S_z|=2$ cannot couple to the light field, and are therefore optically inactive (dark excitons), while states with $|S_z|=1$ are optically active (bright excitons). Bright and dark excitons are split by the (short-range) electron-hole exchange interactions (singlet-triplet splitting $\Delta_{st}$). An external magnetic field $\vec{B}$ causes a further splitting of the excitonic subbands (by the Zeeman interaction) depending on the magnetic field orientation, see Appendix. For semi-magnetic QWs and moderate B ($\sim$T), the Zeeman energies are much larger than an exchange energy $\Delta_{st}$ which is typical of a few tenth of meV.

### A. Faraday geometry

In the presence of a longitudinal magnetic field ($\vec{B}\|z$) both the bright and dark excitons are split by the Zeeman energies which are determined by the electron and hole (longitudinal) $g$ factors, $g_{e,z}$ and $g_{h,z}$. No mixing between the bright and dark states occurs in this case. We consider spin-flip transitions within optically active states from the $|-\frac{3}{2},\frac{1}{2}\rangle$ ($|-1\rangle$) upper spin state with the center-of-mass momentum $\vec{K}$ to the $|\frac{3}{2},-\frac{1}{2}\rangle$ ($|+1\rangle$) lower spin state with the momentum $\vec{K}'$, see Fig. 1(a). Such a transition is a result of two second-order processes, each of them being a first-order process in the exciton-phonon coupling and the coupling of exciton spin states: see Fig. 1(b). Only bright exciton states are involved in the processes above.[27]

The total relaxation rate at zero temperature is

$$W_{sf}=\frac{2\pi}{\hbar}\sum_{\vec{q},\vec{K}'}|M^{\vec{q}}_{-1,K\to+1,K'}|^2\delta(A_hK'^2+\hbar\Omega_{\mathrm{LO}}-E_Z-A_hK^2), \tag{1}$$

where $E_Z$ is the Zeeman energy for the bright exciton, $\hbar\Omega_{\mathrm{LO}}$ and $\vec{q}=\{\vec{Q},q_z\}$ are the LO phonon energy and momentum ($\vec{Q}$ and $q_z$ in the plane and the growth direction of a QW, respectively), $A_h=\hbar^2/2M$ is the exciton band dispersion parameter, the exciton mass is $M=m_e+m_{hh}$, and $m_{hh}$ is an in-plane *hh* mass. We use dispersionless LO phonons to a good approximation since the exciton energy band displays, evidently, a much stronger dispersion than the optical phonon band. The transition matrix element is

$$M^{\vec{q}}_{-1,K\to+1,K'}=\frac{1}{E_Z}[\langle-1|W^{\vec{K}}_{exc}|+1\rangle\langle\vec{K}|U^{\vec{q}}_{ph}|\vec{K}'\rangle-\langle\vec{K}|U^{\vec{q}}_{ph}|\vec{K}'\rangle \times\langle-1|W^{\vec{K}'}_{exc}|+1\rangle], \tag{2}$$

where $\langle\vec{K}|U^{\vec{q}}_{ph}|\vec{K}'\rangle$ is the exciton-phonon scattering matrix element and $\langle-1|W^{\vec{K}}_{exc}|+1\rangle$ is the exchange interaction matrix element, see below. The exciton state is $|\pm1,\vec{K}\rangle=|\pm1\rangle\Psi_{\vec{K}}(\vec{r}_e,\vec{r}_h)$ where $\Psi_{\vec{K}}(\vec{r}_e,\vec{r}_h)$ is the (ground state) exciton envelope wave function, indices $e$ and $h$ stand for electron and hole.

To simplify matters, we perform our calculations under the following conditions.

(i) We assume that the *hh* and *lh* subbands are well separated (due to the confinement and the lattice mismatch-induced strain in the growth direction) compared to the Zeeman splittings, so that the *hh*-*lh* mixing can be neglected. For the *hh* exciton, the subband envelope wave function is separated into a product of electron and hole subband states for the growth direction and a component for the in-plane motion, which we assume to be two-dimensional exciton states:[24]

$$\Psi_{\vec{K}}(\vec{r}_e,\vec{r}_h)=\sqrt{\frac{8}{\pi a_{ex}^2}}e^{-2\rho/a_{ex}}e^{i\vec{K}\vec{R}}\zeta_e(z_e)\zeta_h(z_h). \tag{3}$$

Here, $a_{ex}$ is the (bulk) exciton Bohr radius and $\vec{\rho}$ and $\vec{R}$ are two-dimensional vectors describing the relative and the center-of-mass motion of excitons, respectively. For the motion in the confining direction ($0\leqslant z\leqslant L$), we use an infinite (hard-wall) potential approximation: $\zeta_e(z)=\zeta_h(z)\equiv\zeta(z)=\sqrt{2/L}\sin(\pi z/L)$.

(ii) For the considered case, the Fröhlich interaction of bulk LO phonons with carriers is dominant, so that the exciton-phonon coupling matrix is given by[29,30]

$$\langle \vec{K}|U_{ph}^{\vec{q}}|\vec{K}'\rangle = i\sqrt{\frac{2\pi e^2\hbar\Omega_{\rm LO}(1/\varepsilon_\infty - 1/\varepsilon_0)}{V(q_z^2+Q^2)}} \times\langle\Psi_{\vec{K}}(\vec{r}_e,\vec{r}_h)|e^{i\vec{q}\vec{r}_e} - e^{i\vec{q}\vec{r}_h})|\Psi_{\vec{K}'}(\vec{r}_e,\vec{r}_h)\rangle, \quad (4)$$

where $V$ is the system volume, $\varepsilon_0$ and $\varepsilon_\infty$ denote the static and high-frequency limits of the dielectric function. For the exciton-phonon scattering process, the total in-plane momentum is conserved: $\langle\vec{K}|U_{ph}^{\vec{q}}|\vec{K}'\rangle \propto \delta_{\vec{K}',\vec{K}-\vec{Q}}$. Note that for the phonon-related exponential functions, the following expressions hold:

$$e^{i\vec{q}\vec{r}_e} = e^{iq_z z_e}e^{i\vec{Q}\vec{R}}e^{i\vec{Q}(\mu/m_e)\vec{\rho}},$$

$$e^{i\vec{q}\vec{r}_h} = e^{iq_z z_h}e^{i\vec{Q}\vec{R}}e^{-i\vec{Q}(\mu/m_{hh})\vec{\rho}}, \quad (5)$$

where $\mu = m_e m_{hh}/(m_e+m_{hh})$ is the reduced exciton mass.

(iii) Maialle *et al.*[24] have shown that both the short- and long-range exchange interactions contribute to the coupling of excitonic spin states in a QW, but the latter one is typically dominant. As a result, the matrix element of the (long-range) exchange interaction acting on the spins of the *hh*-exciton ground state is given by [see Eq. (3.4) in Ref. 24]

$$\langle +1|W_{exc}^{\vec{K}}|-1\rangle = \Delta_{LT} f(K)\frac{(K_x - iK_y)^2}{K}, \quad (6)$$

where $\Delta_{LT}$ is the longitudinal-transversal splitting, $K=|\vec{K}|$, and the form factor is

$$f(K) = \frac{3}{2}a_{ex}\int dz \int dz'\,\zeta^2(z)\zeta^2(z')e^{-K|z-z'|}. \quad (7)$$

(iv) Finally, we introduce the following dimensionless parameters:

$$\varepsilon = \frac{E_Z - \hbar\Omega_{\rm LO}}{A_h/a_{ex}^2}, \quad \tilde{\Delta}_{\rm LT} = \frac{\Delta_{\rm LT}}{A_h/a_{ex}^2},$$

$$\kappa = \frac{e^2 a_{ex}}{A_h}(1/\varepsilon_\infty - 1/\varepsilon_0), \quad (8)$$

characterizing the strength of the phonon detuning, the long-range exchange interaction, and the Fröhlich coupling, respectively.

*(a) Zero-momentum excitons*. We consider first the spin-flip transitions from the $K=0$ upper spin state to the $K'\neq 0$ lower spin state of the *hh* exciton. A similar situation is realized in the hot–exciton luminescence experiments in Ref. 22 for (ZnMnSe) DMS layers. In this experiment, the upper spin state of the DMS *hh* exciton is selectively generated by $\sigma^-$-polarized light at $K=0$, see Fig. 2(a). The polarization of a hot PL line opposite to that of the pumping light (i.e., of the same sign as the lower spin state), is observed when the splitting of excitonic subbands $E_Z$ exceeds the LO phonon energy $\hbar\Omega_{\rm LO}$. The energy position of a hot PL line in this case is exactly at one LO phonon energy below the pumping energy. These observations clearly indicate an efficient exciton spin relaxation at $E_Z > \hbar\Omega_{\rm LO}$ when the spin-flip process is accompanied by the emission of one LO phonon. Indeed,

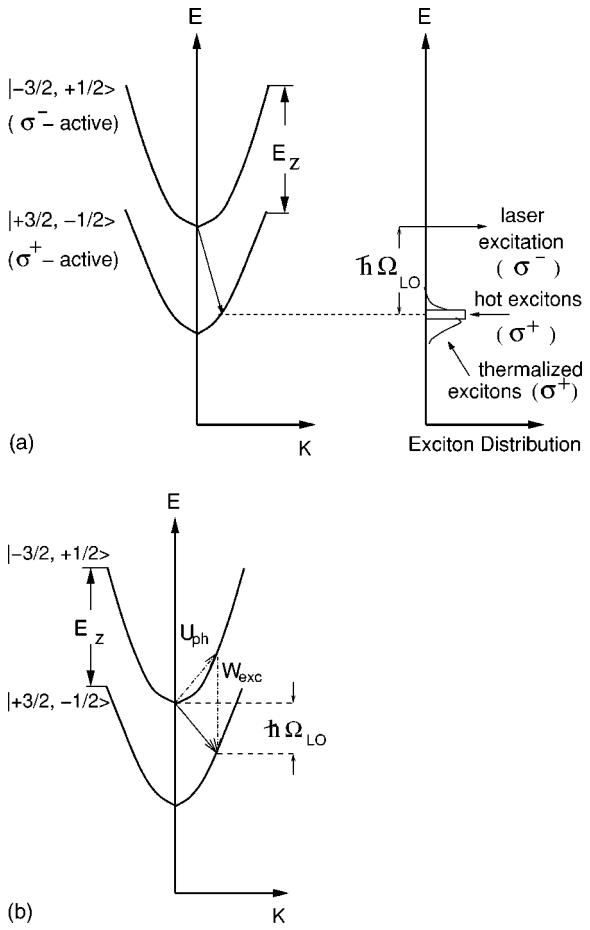


FIG. 2. Schematic diagram showing (a) the two optically active *hh* exciton bands of the DMS QW in $K$ space and the exciton energy distribution under optical pumping in the hot PL experiments according to Ref. 22 and (b) the LO phonon-induced spin-flip process.

if LO-assisted spin relaxation from the upper state with a momentum $K=0$ is allowed, the states in the lowest exciton band with a momentum $K\neq 0$ become occupied resulting in a sharp hot PL line which is fully $\sigma^+$ polarized.

For $K=0$, only the second term in Eq. (2) contributes since there is no coupling between exciton spin states with zero center-of-mass momentum. The corresponding relaxation process is sketched in Fig. 2(b) where the $U_{ph}$ and $W_{ex}$ determine the exciton-phonon coupling and the (exchange-induced) coupling of exciton spin states, respectively.

After some algebra, we obtain the following result:

$$W_{sf}(\varepsilon) = W_0\Phi(\varepsilon)\Theta(\varepsilon), \quad (9)$$

$$W_0 = \frac{9}{8\pi}\Omega_{\rm LO}\tilde{\Delta}_{\rm LT}^2\kappa, \quad (10)$$

$$\Phi(\varepsilon) = \frac{L}{a_{ex}}\frac{\varepsilon}{(\varepsilon+e_0)^2}\Phi_1^2(\varepsilon)\Phi_2^2(\varepsilon)\Phi_3(\varepsilon), \quad (11)$$

where

$$\Phi_1(x) = 64[f_h(x) - f_e(x)], \quad (12)$$

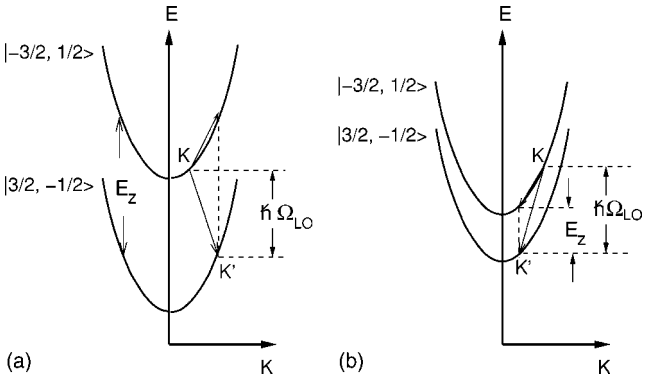


FIG. 3. Schematic illustration to Eq. (19) showing the LO phonon-induced transitions of the *hh* exciton with a momentum $\vec{K}$ (a) antiparallel to the phonon momentum $\vec{Q}$ ($\cos\varphi=-1$), relaxation occurs at $E_Z>\hbar\Omega_{\mathrm{LO}}$, and (b) parallel to $\vec{Q}$ ($\cos\varphi=1$), relaxation occurs at $E_Z<\hbar\Omega_{\mathrm{LO}}$.

$$f_h(x)=(16+xm_{hh}^2/M^2)^{-3/2}, \tag{13}$$

$$f_e(x)=(16+xm_e^2/M^2)^{-3/2}, \tag{14}$$

$$\Phi_2(x)=\frac{4}{\pi^2}\int_0^{\pi}d\xi\sin^2\xi\int_0^{\pi}d\eta\sin^2\eta f(\xi,\eta), \tag{15}$$

$$f(\xi,\eta)=e^{-\sqrt{x}|\xi-\eta|L/\pi a_{ex}}, \tag{16}$$

$$\Phi_3(x)=\int_0^{\infty}dy\frac{g^2(y)}{y^2+xL^2/a_{ex}^2}, \tag{17}$$

$$g(y)=\left(\frac{1}{y}+\frac{y}{\pi^2-y^2}\right)\sin y. \tag{18}$$

Here, the dimensionless energy is $e_0=\hbar\Omega_{\mathrm{LO}}a_{ex}^2/A_h$ and $\Theta(\varepsilon)$ is the step function.

*(b) Hot excitons*. Let us now consider exciton states in the upper spin branch with a finite center-of-mass momentum $K$. For such states, spin-flip transitions occur even when the Zeeman splitting is smaller than the LO phonon energy. From momentum and energy conservation [see Eq. (1)], we have

$$E_Z-\hbar\Omega_{\mathrm{LO}}+2A_hKQ\cos\varphi\equiv A_hQ^2>0, \tag{19}$$

where $\varphi$ is the angle between the exciton and phonon momenta $\vec{K}$ and $\vec{Q}$, respectively. Hence phonons with momentum $\vec{Q}$ in forward direction ($\cos\varphi>0$) with respect to $\vec{K}$ contribute to the spin-flip events at $E_Z<\hbar\Omega_{\mathrm{LO}}$; see Fig. 3.

Hot photoluminescence experiments combined with tunable excitation spectroscopy indicate that spin-preserving energy relaxation of excitons (typically around 1 ps[22]) precedes interband spin-flip transitions in CdSe/ZnMnSe superlattices.[23] Experimental results presented in Ref. 23 refer to the case when the LO phonon energy exceeds the spin splitting (i.e., the phonon detuning is negative, $\varepsilon<0$). For this case, a strong suppression of spin relaxation was observed for small values of exciton momenta.[23]

Using the assumptions (i)–(iv), we found that the exciton spin relaxation rate for $K\neq 0$ is still described by the characteristic rate $W_0$, Eq. (10), but displays a rather intricate dependence on $\varepsilon$ and $K$. As an illustration, we consider the contribution of the $\vec{Q}\|\vec{K}$ ($\varphi=0$) phonons for which the relaxation rate is given by

$$W_{sf}^{\|}(\varepsilon,k)=W_0\frac{F_2(\varepsilon,k)^2}{\sqrt{\varepsilon+k^2}}\times\begin{cases}q_1F(q_1^2)\Theta(\varepsilon), & \varepsilon>0,\\ \sum_{i=1,2}q_iF(q_i^2)\Theta(\varepsilon+k^2), & \varepsilon<0,\end{cases} \tag{20}$$

where dimensionless momentum is $k=(Ka_{ex})$ and

$$F(x)=\frac{L}{2\pi a_{ex}}\frac{1}{(\varepsilon+e_0)^2}\Phi_1^2(x)\Phi_3(x), \tag{21}$$

$$F_2(\varepsilon,k)=\Phi_2(k^2)k-\Phi_2(\varepsilon+k^2)\sqrt{\varepsilon+k^2}, \tag{22}$$

$$q_{1,2}=k\pm\sqrt{\varepsilon+k^2}. \tag{23}$$

Functions $\Phi_j(x)$ are defined by Eqs. (12)–(18).

### B. Voigt geometry

The eigenstates and energies of the ($\vec{K}=0$) *hh* exciton in a titled magnetic field $\vec{B}$ are calculated in the Appendix and are shown schematically in Fig. 5. In transverse magnetic fields ($\vec{B}\perp z$), the *hh* exciton band is split into the two Zeeman subbands, each are twofold degenerate. The Zeeman splitting $E_\perp=|g_{e,\perp}|\mu_BB$ is determined by the transverse electron $g$ factor, $g_{e,\perp}$, since the *hh* spin is locked along the (growth) $z$ axis due to the lifting of *lh-hh* degeneracy by confinement and strain.[31] The excitons with $S_z=-1$ ($S_z=+1$) and $S_z=-2$ ($S_z=+2$) are hybridized and the upper state and the lower state can be excited by both the $\sigma^-$- and $\sigma^+$-polarized light. The phonon-induced relaxation, however, occurs only within the states of the opposite polarization. The spin relaxation rate has the same structure as for the case of Faraday geometry. According to Eq. (A13), it is given (for zero-momentum excitons) by

$$W_{sf}(\varepsilon_\perp)=\frac{W_0}{4}\Phi(\varepsilon_\perp)\Theta(\varepsilon_\perp), \tag{24}$$

$$\varepsilon_\perp=\frac{E_\perp-\hbar\Omega_{\mathrm{LO}}}{A_h/a_{ex}^2}, \tag{25}$$

where the function $\Phi(x)$ is defined by Eqs. (11)–(18).

## III. DISCUSSION

In Eq. (9) for the relaxation rate of excitons with $K=0$ the step function $\Theta(\varepsilon)$ indicates that the spin-flip transitions are only possible when the spin-splitting exceeds the LO phonon energy ($\varepsilon>0$). Likewise, the step function $\Theta(\varepsilon+k^2)$ in Eq.

(20) indicates that for $K \neq 0$ the spin-flip transitions are allowed already at $\varepsilon < 0$, but when $k^2 > |\varepsilon|$ $(\vec{K} \| \vec{Q})$.

According to Eq. (10), the characteristic relaxation rate $W_0$ is determined by the material parameters, in particular, by the longitudinal-transversal splitting $\Delta_{\mathrm{LT}}$ and the Fröhlich coupling $(1/\varepsilon_\infty - 1/\varepsilon_0)$. The relaxation rates (9) and (20) depend also on the electron and the *hh* (in-plane) mass via the function $\Phi_1(x)$ as given Eq. (13). This function tends to zero with $m_e \to m_{hh}$, due to the exciton neutrality. We conclude that DMS's based on $A_{II}B_{VI}$ semiconductors [with typical values of $\Delta_{\mathrm{LT}} \sim 1$ meV, $(1/\varepsilon_\infty - 1/\varepsilon_0) \sim 0.1$, and $m_{hh}/m_e \sim 10$] display faster (LO phonon-induced) exciton spin relaxation than DMS's based on $A_{III}B_V$ semiconductors [with typical values of $\Delta_{\mathrm{LT}} \sim 0.1$ meV, $(1/\varepsilon_\infty - 1/\varepsilon_0) \sim 0.01$, and $m_{hh}/m_e \sim 1$].

Here, we estimate the dependence of the relaxation rates on the phonon detuning parameter $\varepsilon$ and the (dimensionless) exciton momentum $k = Ka_{ex}$. Note that $\Phi_2(x) \sim 1$ for $L \ll a_{ex}$, whereas $\Phi_3(x) \sim 1/\sqrt{x}$. As a result, we find for $k = 0$ (and $m_e \ll m_{hh}$)

$$W_{sf}(\varepsilon) \sim \begin{cases} \varepsilon^2\sqrt{\varepsilon}, & \varepsilon < 1, \\ (\varepsilon\sqrt{\varepsilon})^{-1}, & \varepsilon > \max\{\omega_0, 16\}, \end{cases} \tag{26}$$

whereas for large $k \gg \sqrt{|\varepsilon|}$

$$W_{sf}^{\|}(\varepsilon, k) \sim \begin{cases} \varepsilon^2 k^{-5}, & \varepsilon < 1, \\ k^{-5}, & \varepsilon > \max\{\omega_0, 16\}. \end{cases} \tag{27}$$

Note that the exciton momenta are effectively limited by $K_{\max} = \sqrt{\hbar\Omega_{\mathrm{LO}}/A_h}$ $(k_{\max} = \sqrt{e_0})$ when the spin-flip relaxation is slower than the spin-preserving one. In this case, for an exciton with a momentum $K \geqslant K_{\max}$ (and hence with an energy equal or larger than $\hbar\Omega_{\mathrm{LO}}$), the relaxation occurs more likely within the upper spin band, by an emission of one LO phonon, than to the lower spin band.

For numerical calculations, we use the material parameters for ZnSe crystals adopted from Ref. 32: $\hbar\Omega_{\mathrm{LO}} = 32$ meV, $\Delta_{\mathrm{LT}} = 2$ meV, $m_e = 0.13m_0$, $m_{hh} = 0.52m_0$, $a_{ex} = 4.5$ nm, $\varepsilon_0 = 9.6$, and $\varepsilon_\infty = 5.4$ (dimensionless energy is $e_0 \simeq 12$). The relaxation rate $W_{sf}(\varepsilon)$ calculated with Eqs. (9)–(16) is shown in Fig. 4(a) as a function of $\varepsilon$: $W_{sf}(\varepsilon)$ increases with $\varepsilon > 0$ and saturates at $\varepsilon \sim 10-15$. Also, for a fixed value of $\varepsilon$, the relaxation rate is larger in QWs with a small width $L$ than for larger $L$ due to the raising of the exchange interaction Eq. (6).

Evaluation of the relaxation time $W_{sf}^{\|}(\varepsilon, k)$ [calculated with Eqs. (20)–(23)] is shown in Fig. 4(b). (For the above material parameters, $k_{\max} = \sqrt{e_0} \simeq 3.4$.) The relaxation rate $W_{sf}^{\|}$ decreases with an increase of $k$ and is almost independent of $\varepsilon$ at large momenta near $k \sim 3$.

According to our numerical results presented in Figs. 4, we conclude that zero-momentum excitons display the most efficient (LO phonon-induced) spin relaxation in thin QWs which have spin-splittings larger than the LO phonon energy. For the ZnSe-based semimagnetic QWs of $L \sim 3$ nm, for example, the spin relaxation time drops from $\sim 50$ ps at $(E_Z - \hbar\Omega_{\mathrm{LO}}) \sim 9$ meV to $\sim 12$ ps at $(E_Z - \hbar\Omega_{\mathrm{LO}}) \sim 40$ meV. Experimental findings in Ref. 22 refer to the well width of $L$

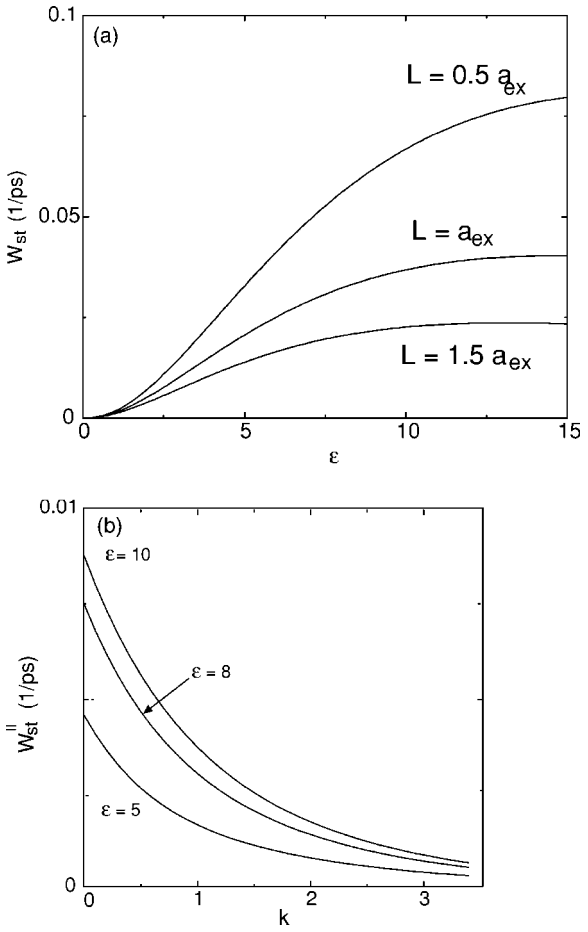


FIG. 4. Calculated exciton spin-flip relaxation rate as a function of (a) the phonon detuning parameter $\varepsilon$ at $k = 0$ and (b) the (dimensionless) exciton momentum $k$ at $\varepsilon > 0$, $L = 0.5a_{ex}$. (For material parameters given in text, the energy difference is $E_Z - \hbar\Omega_{\mathrm{LO}} \simeq 2.9\varepsilon$ meV.)

$\sim 10$ nm and the energy difference of $(E_Z - \hbar\Omega_{\mathrm{LO}}) \sim 10$ meV. For such parameters, we obtain the spin lifetime of $\sim 70$ ps. A direct quantitative comparison of our proposed model to experiments[22,23] is, unfortunately, hardly possible, since no spin relaxation times are given. Trends as well as numerical estimates of our model agree qualitatively well with the experimental findings. The value of the spin relaxation time between the spin-preserving relaxation (around 1 ps) and the decay rate of the DMS exciton (around tens of ps) is reproduced. We correctly explain the experimental findings that spin relaxation is strongly suppressed for excitons with a small momentum when the spin-splitting is smaller than the LO phonon energy.

For Zn(Cd)Se-based semimagnetic QWs, Faraday geometry is mostly favorable, since the spin splitting is much larger at $\vec{B} \| z$ than at $\vec{B} \perp z$ in these structures. The reason is that the strength of the exchange interaction with magnetic ions is larger for holes[28] than for electrons resulting in a large $g_{h,z}$ and $E_Z$ compared to $g_{e,z}$ $(\sim g_{e,\perp})$ and $E_\perp$, respectively. Therefore an efficient (LO) phonon-induced spin relaxation in a longitudinal magnetic field will be totally suppressed by the change of the magnetic field orientation from $\vec{B} \| z$ to $\vec{B} \perp z$.

Within our model of direct spin-flip transitions (Faraday geometry), the exciton spin-relaxation rate $W_{sf}$ depends strongly on a magnetic field, in particular, because of the phonon density of states. A strong *monotonic* increase in the relaxation occurs when the exciton spin-splitting starts to exceed the LO phonon energy, i.e., at small $\varepsilon$. For hot excitons, $W_{sf}$ decreases with an increase of the center-of-mass momentum $K$. Different results can be expected for spin-flip transitions mediated by the spin scattering via magnetic ions. Namely, a *steplike* dependence on $\varepsilon$ (at small $\varepsilon$), and an increase with $K$ must be typical in this case. Indeed, the magnetic exchange-induced spin-relaxation is a result of combined spin-flip processes (which are almost elastic because of the small Zeeman splitting of magnetic ions) and the LO-assisted energy relaxation process within the lowest excitonic band.[22] The latter (spin-preserving) process is independent of the spin-splitting, except that it starts at $E_Z > \hbar\Omega_{\mathrm{LO}}$, i.e., at $\varepsilon > 0$. Since the hole spin-flip process requires the *hh*-*lh* mixing,[13] the former process is more efficient the larger $K$ is.[33] In addition, the well width dependence is different, namely, the calculated here relaxation rates increase when L decreases, while for the spin relaxation by the magnetic scattering the opposite trend is typical due to the reduction of the valence-band mixing.

The spin relaxation dependence on spin-splitting of the DMS exciton was studied in Ref. 22 by optical spin injection experiments in CdSe/ZnMnSe superlattices. It was found that spin relaxation exhibits a pronounced increase when the energy separation of the two spin states crosses the LO phonon energy. The change in spin relaxation in this region is rather *monotonic* than of a step type. The time-resolved Faraday rotation experiments indicate, however, the dominant role of the carrier-magnetic ions spin-flip interactions in (Zn-,Mn,Cd)Se QWs. The spin-relaxation times of the same order were deduced for the excitons (Faraday geometry) and the electrons or holes (Voigt geometry) in these experiments.[7] More measurements are necessary in order to test further the theory, looking, e.g., at the magnetic-field dependence of $W_{sf}$.

## IV. CONCLUSIONS

Our intent has been to point out the importance of direct spin-flip transitions within exciton subbands (split by external magnetic field) in semimagnetic quantum wells. The exciton-spin relaxation is considered in terms of the coupling between exciton spin states with a finite center-of-mass momentum via the electron-hole exchange interaction in a QW (the MAS mechanism). A specific case of spin-splittings larger than the LO phonon energy is considered and the relaxation is induced by LO phonons. The proposed mechanism is also relevant for the opposite case of small spin-splittings when (instead of optical phonons) acoustic phonons come into play.[34] The phonon-induced relaxation considered here is similar to the Elliott-Yafet mechanism[35,36] for the electron relaxation in metals and semiconductors.[37] Note that the MAS mechanism dominates the exciton spin relaxation for conventional quantum wells.[24] The spin dynamics in this case, however, is analogous to the one observed in the motional narrowing effect in nuclear spin relaxation in metals[38] and also in the Dyakonov-Perel mechanism for the electron spin relaxation in bulk semiconductors.[39] The motional narrowing type of a spin relaxation is suppressed by an external magnetic field (along the growth direction),[24] in contrast to the case considered here.

Our results explain qualitatively the experimental findings that spin relaxation is strongly suppressed for excitons with a small momentum when the spin-splitting is smaller than the LO phonon energy.[22,23] The rates increase strongly with a magnetic field and they decrease with the exciton momentum, findings that would be interesting to verify experimentally. They also depend on material. For example, $W_{sf} \sim \Delta_{\mathrm{LT}}^2$, where $\Delta_{\mathrm{LT}}$ is the longitudinal-transversal splitting. Thus, for DMS's based on the $A_{II}B_{VI}$ semiconductors ($\Delta_{\mathrm{LT}} \sim 1$ meV) spin relaxation rates will be orders of magnitude larger than those for DMS's based on the $A_{III}B_{V}$ semiconductors ($\Delta_{\mathrm{LT}} \sim 0.1$ meV). The rates are relatively low at small phonon detuning $E_Z \gtrsim \hbar\Omega_{\mathrm{LO}}$, but $\sim$20 picoseconds can be achieved at $E_Z \sim 2\hbar\Omega_{\mathrm{LO}}$, e.g., in ZnSe-based quantum wells with a width $L \sim 5$ nm. These values lie between the spin-preserving relaxation (around 1 ps) and the decay rate of the DMS exciton (around tens of ps). For Zn(Cd)Se-based semimagnetic QWs in transverse (modest) magnetic fields, the (LO) phonon-induced exciton spin relaxation is strongly suppressed due to the small Zeeman splittings compared to the LO phonon energy.

## ACKNOWLEDGMENTS

We thank E. L. Ivchenko for helpful discussions. This work was supported by the Center for Functional Nanostructures (CFN) of the Deutsche Forschungsgemeinschaft (DFG) within project A2.

## APPENDIX: TITLED MAGNETIC FIELD

For the *hh* exciton, the main part of the spin-related Hamiltonian (small exchange- and magnetic field-induced terms are neglected) is given by[26]

$$H = -\frac{2}{3}\Delta_{st}\vec{J}\vec{\sigma} + \frac{1}{2}\mu_B\left[(g_{e,z}\sigma_z B_z + g_{e,\perp}\vec{\sigma}_\perp\vec{B}_\perp) + \frac{1}{3}g_{h,z}J_z B_z\right], \tag{A1}$$

where the first term stands for the electron-hole (short-range) exchange interaction, and $\Delta_{\mathrm{st}}$ is the (singlet-triplet) exchange energy. Terms in the square brackets stand for the interaction of the electron and hole spins with an external magnetic field $\vec{B} = B(\cos\varphi\sin\theta, \sin\varphi\sin\theta, \cos\theta)$, $\mu_B$ is the Bohr magneton, and $g_{e,z}$ ($g_{e,\perp}$) and $g_{h,z}$ is the electron and hole gyromagnetic ratio ($g$ factor), respectively. $\vec{J}$ is the hole total angular momentum (spin), $\sigma_z$, and $\vec{\sigma}_\perp(\sigma_x, \sigma_y)$ are the Pauli matrices.

In the basis of the *hh*-exciton states ($|-1\rangle$, $|-2\rangle$, $|+1\rangle$, and $|+2\rangle$), the Hamiltonian (A1) is represented by the following matrix:

$$H=\frac{1}{2}\mu_B B\begin{pmatrix}(g_{e,z}+g_{h,z})\cos\theta+\Delta_{st} & g_{e,\perp}e^{-i\varphi}\sin\theta & 0 & 0\\ g_{e,\perp}e^{i\varphi}\sin\theta & (g_{h,z}-g_{e,z})\cos\theta & 0 & 0\\ 0 & 0 & -(g_{e,z}+g_{h,z})\cos\theta+\Delta_{st} & g_{e,\perp}e^{i\varphi}\sin\theta\\ 0 & 0 & g_{e,\perp}e^{-i\varphi}\sin\theta & (g_{e,z}-g_{h,z})\cos\theta\end{pmatrix}, \tag{A2}$$

The matrix (A2) has a block diagonal form, so that the eigenstates and their energies can be easily obtained. Generally, the excitons with $S_z=-1$ ($S_z=+1$) and $S_z=-2$ ($S_z=+2$) are hybridized and the spectrum is fully split by Zeeman interaction. For Faraday geometry ($\theta=0$), the eigenstates reduce to the pure spin states of the bright and dark excitons, while for Voigt geometry ($\theta=\pi/2$), the spectrum remains twofold degenerate.

For the relevant case of the large Zeeman splittings compared to the exchange energy $\Delta_{st}$ ($\Delta_{st}\sim 0.3$ meV is typical, e.g., for ZnSe-based semimagnetic QWs[7]) and an isotropic electron $g$ factor, the eigenstates are

$$\Psi_1^{(+)}=\frac{1}{\sqrt{2}}[e^{-i\varphi/2}b_+|-1\rangle-e^{i\varphi/2}b_-|-2\rangle], \tag{A3}$$

$$\Psi_2^{(+)}=\frac{1}{\sqrt{2}}[e^{i\varphi/2}b_-|1\rangle-e^{-i\varphi/2}b_+|2\rangle], \tag{A4}$$

$$\Psi_1^{(-)}=\frac{1}{\sqrt{2}}[e^{i\varphi/2}b_+|1\rangle+e^{-i\varphi/2}b_-|2\rangle], \tag{A5}$$

$$\Psi_2^{(-)}=\frac{1}{\sqrt{2}}[e^{-i\varphi/2}b_-|-1\rangle+e^{i\varphi/2}b_+|-2\rangle], \tag{A6}$$

where $b_\pm=\sqrt{1\pm\cos\theta}$. The corresponding energies are

$$E_1^{(+)}=-E_1^{(-)}=\frac{1}{2}\mu_B B(g_{h,z}\cos\theta+g_e), \tag{A7}$$

$$E_2^{(+)}=-E_2^{(-)}=\frac{1}{2}\mu_B B(-g_{h,z}\cos\theta+g_e), \tag{A8}$$

where $g_e=g_{e,z}=g_{e,\perp}$.

For Faraday geometry ($\theta=0$), Zeeman splittings are determined by both the electron and hole $g$ factors: $E_Z=|E_1^{(+)}-E_1^{(-)}|=|g_e+g_{h,z}|\mu_B B$ and $E_Z^{dark}=|E_2^{(+)}-E_2^{(-)}|=|g_e-g_{h,z}|\mu_B B$ for bright and dark excitons, respectively. For Voigt geometry ($\theta=\pi/2$), the *hh* exciton splits into two levels, each twofold degenerate. The Zeeman splitting is determined by the electron $g$ factor only: $E_\perp=|E_1^{(+)}-E_1^{(-)}|\equiv|E_2^{(+)}-E_2^{(-)}|=|g_e|\mu_B B$.[26] For the specific case of the ZnSe-based semimagnetic QWs ($g_{h,z}>0$, $g_e>0$, and $g_{h,z}>g_e$[28]), the energies Eqs. (A7) and (A8) are shown in Fig. 5.

One readily checks that the matrix elements of the exciton-phonon interaction vanishes, $\langle\Psi_1^{(\pm)}|U_{ph}|\Psi_2^{(\mp)}\rangle=0$, $\langle\Psi_1^{(\pm)}|U_{ph}|\Psi_2^{(\pm)}\rangle=0$, $\langle\Psi_{1,2}^{(+)}|U_{ph}|\Psi_{1,2}^{(-)}\rangle=0$, so that there are no phonon-induced spin-preserving transitions between Zeeman subbands. In other words, the spin-independent perturbation does not couple the states (A3)–(A6) with one other. The following states are mixed via the long-range exchange interaction (which mixes the $S_z=1$ states only[24]):

$$\langle\Psi_{1,\vec{K}}^{(-)}|W_{exc}^{\vec{K}}|\Psi_{1,\vec{K}}^{(+)}\rangle=\frac{e^{-i\varphi}}{2}b_+^2\langle 1|W_{exc}^{\vec{K}}|-1\rangle, \tag{A9}$$

$$\langle\Psi_{2,\vec{K}}^{(+)}|W_{exc}^{\vec{K}}|\Psi_{2,\vec{K}}^{(-)}\rangle=\frac{e^{-i\varphi}}{2}b_-^2\langle 1|W_{exc}^{\vec{K}}|-1\rangle, \tag{A10}$$

$$\langle\Psi_{2,\vec{K}}^{(+)}|W_{exc}^{\vec{K}}|\Psi_{1,\vec{K}}^{(+)}\rangle=\frac{e^{-i\varphi}}{2}b_-b_+\langle 1|W_{exc}^{\vec{K}}|-1\rangle, \tag{A11}$$

$$\langle\Psi_{1,\vec{K}}^{(-)}|W_{exc}^{\vec{K}}|\Psi_{2,\vec{K}}^{(-)}\rangle=\frac{e^{-i\varphi}}{2}b_-b_+\langle 1|W_{exc}^{\vec{K}}|-1\rangle, \tag{A12}$$

where the matrix element $\langle 1|W_{exc}^{\vec{K}}|-1\rangle$ is given by Eq. (6) and $\Psi_{i,\vec{K}}^{(\pm)}=\Psi_i^{(\pm)}\Psi_{\vec{K}}(\vec{r}_e,\vec{r}_h)$.

For Faraday geometry ($b_+=\sqrt{2}$ and $b_-=0$) the exchange-induced mixing occurs, evidently, for bright excitons only. In tilted magnetic fields, however, there are additionally the spin-flip transitions within the states of bright and dark excitons; see Fig. 5. Using the assumptions (i)–(iv) in the main text and expressions (A9)–(A12), we obtain the following result:

$$W_{11}(\theta)=\frac{W_0}{4}b_+^4\Phi(\varepsilon_{11})\Theta(\varepsilon_{11}), \tag{A13}$$

$$W_{12}(\theta)=\frac{W_0}{4}b_+^2b_-^2\Phi(\varepsilon_{12})\Theta(\varepsilon_{12}), \tag{A14}$$

$$\varepsilon_{11}(\theta)=\frac{E_1^{(+)}-E_1^{(-)}-\hbar\Omega_{\mathrm{LO}}}{A_h/a_{exc}^2}, \tag{A15}$$

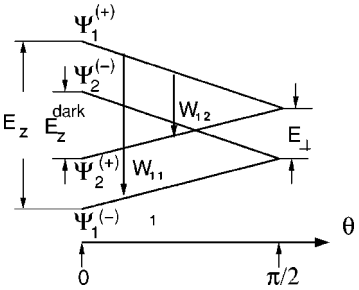


FIG. 5. Schematic illustration to Eqs. (A7) and (A8) showing the energies of the *hh* exciton (K=0) in tilted magnetic field, $g_{h,z}>0$, $g_e>0$ ($g_{e,z}=g_{e,\perp}$).

$$\varepsilon_{12}(\theta) = \frac{E_1^{(+)} - E_2^{(+)} - \hbar\Omega_{\mathrm{LO}}}{A_h/a_{exc}^2}, \tag{A16}$$

where the function $\Phi(x)$ is determined by Eqs. (11)–(18). For both Faraday and Voigt geometry, only one relaxation process survives. For Faraday geometry, the coefficients are $b_+ = \sqrt{2}$ and $b_- = 0$, so that Eq. (A13) reduces to Eq. (9) in the main text and $W_{12}(0) = 0$. For Voigt geometry, the coefficients are $b_+ = b_- = 1$, so that Eq. (A13) reduces to Eq. (24) in the main text and $W_{12}(\pi/2) = 0$, since the phonon detuning parameter $\varepsilon_{12}(\pi/2)$ is negative, $\varepsilon_{12}(\pi/2) = -\hbar\Omega_{\mathrm{LO}} a_{exc}^2/A_h$.

*Permanent address: Institute for Cybernetics, Academy of Science, S. Euli 5, 380086, Georgian Republic.

[1] M. Oestreich, J. Hübner, D. Hägele, P. J. KLar, W. Heimbrodt, W. W. Rühle, D. E. Ashenford, and B. Lunn, Appl. Phys. Lett. **74**, 1251 (1999).
[2] R. Fiederling, M. Keim, G. Reuscher, W. Ossau, G. Schmidt, A. Waag, and L. Molenkamp, Nature (London) **402**, 787 (1999).
[3] See I. A. Buyanova, G. Yu. Rudko, W. M. Chen, A. A. Toropov, S. V. Sorokin, S. V. Ivanov, and P. S. Kop'ev, Appl. Phys. Lett. **82**, 1700 (2003), and references therein.
[4] M. R. Freeman and D. D. Awschalom, J. Appl. Phys. **67**, 5102 (1990).
[5] M. R. Freeman, D. D. Awschalom, J. M. Hong, and L. L. Chang, Phys. Rev. Lett. **64**, 2430 (1990).
[6] S. A. Crooker, J. J. Baumberg, F. Flack, N. Samarth, and D. D. Awschalom, Phys. Rev. Lett. **77**, 2814 (1996).
[7] S. A. Crooker, D. D. Awschalom, J. J. Baumberg, F. Flack, and N. Samarth, Phys. Rev. B **56**, 7574 (1997).
[8] R. Akimoto, K. Ando, F. Sasaki, S. Kobayashi, and T. Tani, Phys. Rev. B **56**, 9726 (1997).
[9] B. Koopmans, M. van Kampen, and W. J. M. de Jonge, Phys. Status Solidi B **215**, 217 (1999).
[10] C. Camilleri, F. Teppe, D. Scalbert, Y. G. Semenov, M. Nawrocki, M. Dyakonov, J. Cibert, S. Tatarenko, and T. Wojtowicz, Phys. Rev. B **64**, 085331 (2001).
[11] C. J. P. Smits, S. C. A. van Driel, M. van Kampen, W. J. M. de Jonge, B. Koopmans, and G. Karczewski, Phys. Rev. B **70**, 115307 (2004).
[12] G. Bastard and L. L. Chang, Phys. Rev. B **41**, R7899 (1990).
[13] R. Ferreira and G. Bastard, Phys. Rev. B **43**, 9687 (1991).
[14] G. Bastard and R. Ferreira, Surf. Sci. **267**, 335 (1992).
[15] Y. G. Semenov, Phys. Rev. B **67**, 115319 (2003).
[16] See, e.g., T. H. Stievater, X. Li, D. G. Steel, D. Gammon, D. S. Katzer, D. Park, C. Piermarocchi, and L. J. Sham, Phys. Rev. Lett. **87**, 133603 (2001).
[17] K. Kayanuma, M. C. Debnath, I. Souma, Z. Chen, A. Murayama, M. Kobayashi, H. Miyazaki, and Y. Oka, Phys. Status Solidi B **229**, 761 (2002).
[18] J. F. Smyth, D. A. Tulchinsky, D. D. Awschalom, N. Samarth, H. Luo, and J. K. Furdyna, Phys. Rev. Lett. **71**, 601 (1993).
[19] W. C. Chou, A. Petrou, J. Warnock, and B. T. Jonker, Phys. Rev. B **46**, R4316 (1992).
[20] B. T. Jonker, L. P. Fu, W. Y. Yu, W. C. Chou, A. Petrou, and J. Warnock, J. Appl. Phys. **73**, 6051 (1993).
[21] C. D. Poweleit, A. R. Hodges, T.-B. Sun, L. M. Smith, and B. T. Jonker, Phys. Rev. B **59**, 7610 (1999) and references therein.
[22] W. M. Chen, I. A. Buyanova, G. Yu. Rudko, A. G. Mal'shukov, K. A. Chao, A. A. Toropov, Y. Terent'ev, S. V. Sorokin, A. V. Lebedev, S. V. Ivanov, and P. S. Kop'ev, Phys. Rev. B **67**, 125313 (2003).
[23] I. A. Buyanova, G. Yu. Rudko, and W. M. Chen, J. Appl. Phys. **93**, 7352 (2002).
[24] M. Z. Maialle, E. A. de Andrada e Silva, and L. J. Sham, Phys. Rev. B **47**, 15776 (1993).
[25] For holes, the spin-relaxation rate is $\tau_h^{-1} \sim A_{hl}(\beta^2/\alpha^2)\tau_e^{-1}$, where $\alpha(\beta)$ is the electron (hole) exchange interaction strength. The coefficient $A_{hl}$ is determined by mixing between the heavy-hole (*hh*) and light-hole (*lh*) bands. For ZnMnSe, $\beta \sim 5\alpha$ (Ref. 28) which implies $\tau_h \sim 4\tau_e$ at $A_{hl} \sim 0.01$ [the case when the *hh*-exciton Zeeman splitting is comparable to the (zero-magnetic field) *lh-hh* splitting].
[26] E. L. Ivchenko and G. Pikus, in *Superlattices and Other Heterostructures*, edited by M. Cardona, P. Fulde, K. von Klitzing, and H.-J. Queisser (Springer-Verlag, Berlin, Heidelberg, 1995).
[27] For a two-step relaxation (by an independent change in the electron and hole spin), transitions occur via dark states: $|-1\rangle \rightarrow |-2\rangle \rightarrow |+1\rangle$ (change in the electron spin and then the hole spin), or $|-1\rangle \rightarrow |+2\rangle \rightarrow |+1\rangle$ (change in the hole spin and then the electron spin).
[28] O. Goede and W. Heimbrodt, Phys. Status Solidi B **146**, 11 (1988).
[29] W. Fröhlich, in *Polarons and Excitons*, edited by C. G. Kuper and G. D. Whitfield (Oliver and Boyd, Edinburg, 1963).
[30] R. S. Knox, in *Theory of Excitons*, edited by F. Seitz and D. Turnbull (Academic, New York and London, 1963).
[31] A reorientation of the *hh* spins from the growth direction to the (in-plane) field direction occurs when the Zeeman energies overcome the *hh-lh* splittings; see Ref. 7 and references therein.
[32] Landolt-Börnstein, in *New Series*, edited by O. Madelung, M. Schultz, and H. Weiss (Springer-Verlag, Berlin, 1982), Vol. 17b, Group III.
[33] For hot excitons, an elastic spin-flip process due to the scattering by nonmagnetic potential fluctuations, mediated, e.g., by the MAS exchange coupling, and assisted by an emission of LO phonons in the lower spin subband can be important.
[34] E. Tsitsishvili, R. v. Baltz, and H. Kalt (unpublished).
[35] R. J. Elliott, Phys. Rev. **96**, 266 (1954).
[36] Y. Yafet, in *Solid State Physics*, edited by F. Seitz and D. Turnbull (Academic, New York, 1963), Vol. 14.
[37] For recent review, see I. Žutić, J. Fabian and S. Das Sarma, Rev. Mod. Phys. **76**, 323 (2004).
[38] C. P. Slichter, *Principles of Magnetic Resonance* (Springer, Berlin, 1989).
[39] M. I. D'yakonov and V. I. Perel, Zh. Eksp. Teor. Fiz. **60**, 1954 (1971) [Sov. Phys. JETP **33**, 1053 (1971)]; Fiz. Tverd. Tela (Leningrad) **13**, 3581 (1971) [Sov. Phys. Solid State **33**, 3023 (1972)].